

# Bond Graph Based Sensitivity and Uncertainty Analysis Modelling for Micro-Scale Multiphysics Robust Engineering Design

M. A. Perry,<sup>a,\*</sup> M. A. Atherton,<sup>b</sup> R. A. Bates,<sup>a</sup> H. P. Wynn.<sup>a</sup>

<sup>a</sup>*Dept. of Statistics, London School of Economics, London WC2A 2AE, UK.*

<sup>b</sup>*School of Engineering and Design, Brunel University, UK.*

---

## Abstract

Components within micro-scale engineering systems are often at the limits of commercial miniaturization and this can cause unexpected behavior and variation in performance. As such, modelling and analysis of system robustness plays an important role in product development. Here schematic bond graphs are used as a front end in a sensitivity analysis based strategy for modelling robustness in multiphysics micro-scale engineering systems. As an example, the analysis is applied to a behind-the-ear (BTE) hearing aid.

By using bond graphs to model power flow through components within different physical domains of the hearing aid, a set of differential equations to describe the system dynamics is collated. Based on these equations, sensitivity analysis calculations are used to approximately model the nature and the sources of output uncertainty during system operation. These calculations represent a robustness evaluation of the current hearing aid design and offer a means of identifying potential for improved designs of multiphysics systems by way of key parameter identification.

*Key words:* Bond Graph Modelling; Sensitivity Analysis; Uncertainty Analysis; Hearing Aid Device; Multiphysics; Robustness.

---

---

\* Corresponding author tel/fax +44-207-955-7622/7416 email: m.perry@lse.ac.uk

## 1 Introduction

Robust Engineering Design (RED) refers to the group of methodologies dedicated to reducing the variation in performance of products and processes arising from manufacture and use. In addition to design and analysis of experiments, it now includes computer experiments on CAD/CAE simulation, advanced Response Surface Modelling methods, adaptive optimisation methodologies and reliability analysis, and should be included within general life-cycle design. RED has been shown to be very effective in improving product or process design through its use of experimental design and analysis methods [1] [2]. However, RED has not been fully developed at the micro-scale [3] where statistical variations could be relatively more important.

Hearing aids consist of an assembly of very small components such as telecoils, microphones, receivers and amplifiers. A typical such system is shown in Figure 1. In order to fit in or around the ear and provide high gain, some of these components are at the limits of commercial miniaturization which can cause unexpected behavior and variation in performance. The economic and social cost of hearing loss for the countries of the Europe Union was estimated to be in excess of \$220 billion in 2004 [4]. This highlights the need to develop reliable, robust, high-quality hearing devices. A robustness analysis of a micro-scale behind-the-ear (BTE) hearing aid device is performed in this paper by way of using bond graph modelling alongside analytic sensitivity and uncertainty methods and builds on a related empirical approach [5]. Recent published work on hearing aids [6] has focused on algorithms for improved digital signal processing such as speech enhancement [7], interference cancellation [8] and new technology such as dual microphones [9]. Robustness has only been addressed in terms of feedback. Therefore, to the authors knowledge, the numerical results presented here on hearing aid robustness in terms of physical parameters are new.

A hearing aid works in two modes; microphone mode and telecoil mode. In microphone mode sound is converted into an electrical signal by the microphone, which is then amplified and converted back into sound by a loudspeaker called the receiver. In telecoil mode, instead of detecting sound pressure via a microphone, the sound is transmitted as a radio signal and converted into an

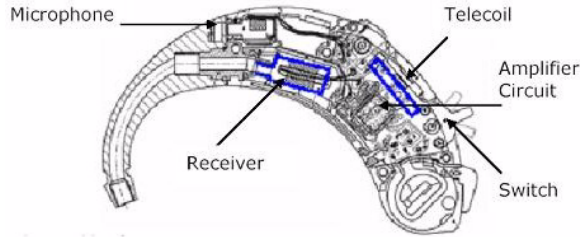


Fig. 1. Assembly diagram of BTE Hearing Aid

electrical signal by the telecoil.

In the work presented here a bond graph model of a hearing aid is developed and used to derive a set of governing differential equations for the system. Solving these equations numerically, in parallel with the corresponding sensitivity differential equations, provides a simulation tool which models system output as well as the sensitivity of this output to parameter variability. Based on an output uncertainty approximation, these sensitivity results facilitate identification of the components whose variability have greatest effect on system performance. The levels of variability in the parameters is pre-defined by the particular product specifications within the manufacturing process.

## 2 Bond Graph Modelling and Equation Generation

Bond graphs, introduced by Paynter [10], can be used to model multi-energy domain systems based on electro-mechanical analogues. Notable contributions to bond graph theory have been made by Karnopp [11], Rosenberg [12] and Cellier [13]. Dynamic physical systems are concerned with one or more of the following: (i) energy transfer, (ii) mass transfer, and (iii) information (or signal) transfer. Bond graphs are an abstract representation of a system that uses one set of symbols to represent all applicable types of systems in terms of energy transfer [14]. In particular, they focus on the exchange of power between components by considering the flow of independent power variables<sup>1</sup> from one energy domain to another. The causality assignment and model-

<sup>1</sup> The power variables are independent of the energy domain through which they flow

building associated with bond graphs makes them an interesting candidate for combination with RED methods, as described by Atherton and Bates [15], who applied bond graph models in an industrial engineering environment to perform RED on the design of both a loudspeaker driver unit and a hedge trimmer. In addition, Atherton et al [5] used bond graph models to perform robustness analysis on the BTE hearing aid using a designed computer experiment. The results demonstrated good agreement between simulation and physical experiments.

The sensitivity bond graph approach [16] develops sensitivity components which model the sensitivity of efforts and flows with respect to changes in component parameter values. These sensitivities are then combined in a bond graph to implicitly solve the system sensitivity equations. In contrast, the method presented here uses bond graphs to obtain a set of *linearized* governing system equations that are the starting point for developing a corresponding sensitivity analysis formulation. All of the equations are then directly solved and analysed outside the bond graph environment. In this way, the techniques used to solve the differential equation systems are not governed by the choice of bond graph simulator. Furthermore, the construction of incremental bond graphs is avoided [17] and the original engineering system topology is maintained. In this paper the linearization process is performed by the bond graph simulator 20-Sim [18]. This translates the bond graph system symbolically into a standard state-space form around a chosen working point. The symbolic linearization requires that all the elements of the original system are differentiable.

Figure 2 shows the bond graph model of the BTE hearing aid device which in this paper is modelled in telecoil mode rather than microphone mode as considered in [5]. In the bond graph representation, the telecoil is represented as a pure inductance by a generalised inertia element,  $I_{coil}$ . Indeed, all the electro-magneto-mechanical elements are represented in electrical terms in this bond graph in accordance with standard industry practice. The signal to the telecoil originates from a radio loop, which is represented as a modulated effort source with a.c. and d.c. parts. The three-stage amplifier is prominent in the center of the bond graph (shaded grey) is represented here, as in [5], in signal terms rather than power transmitting elements. This is because the

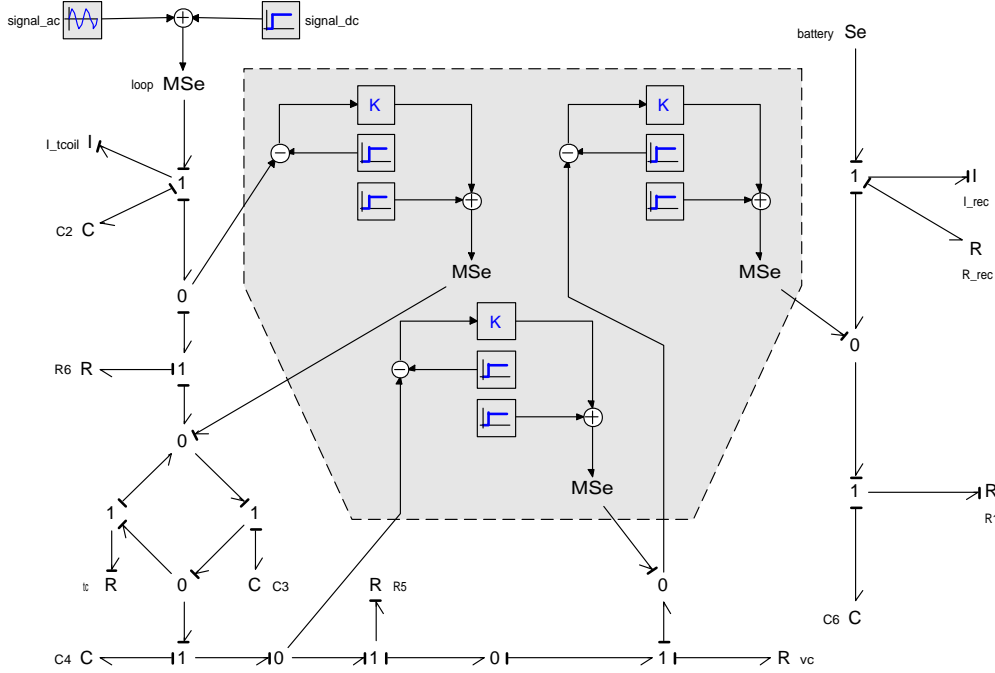


Fig. 2. Bond graph model of a hearing aid device in telecoil mode.

amplifier stage is an integrated circuit and, as this part of the design is not modifiable in practice, it is represented as a set of three simple gain stages (K-blocks). The signal blocks represent either the construction of the test signal, or D.C. shifts to represent the functional behaviour of the amplifier gain stages. Numbered  $R$  and  $C$  elements represent various basic electrical resistors and capacitors of the circuit respectively, and  $R_{tc}$  and  $R_{vc}$  represent tone control and volume control variable resistors respectively. The receiver, which produces sound output, is limited to equivalent circuit load elements,  $R_{rec}$  and  $I_{rec}$ , rather than attempt to model the many component parts associated with generating acoustic output. The resultant bond graph maintains integral causality throughout, thus remaining mathematically well formulated.

The bond graph simulation software 20-sim [18] was used to simulate the model in Figure 2, subject to a sinusoidal input signal  $MS_e$ , and five system state variables were identified from the linearization process, as listed in Table 1. The independent system parameters identified by the bond graph model are presented in Table 2.

One of the advantages of bond graph modelling is the facility to extract the governing system differential equations from the bond graph representation

|                |                          |
|----------------|--------------------------|
| $v_{C_2}(t)$   | Voltage across C2        |
| $v_{C_3}(t)$   | Voltage across C3        |
| $v_{C_4}(t)$   | Voltage across C4        |
| $i_{rec}(t)$   | Current through Receiver |
| $i_{tcoil}(t)$ | Current through Telecoil |

Table 1

System states in bond graph of hearing aid system

by linearization around a working point, determined by solving the nonlinear system and specifying system inputs and outputs. This is achieved by enforcing conservation of power laws at each junction in terms of the independent effort and flow variables, and is performed automatically by the bond graph simulation software [18]. The linearized dynamic governing system differential equations of the system in Figure 2 are generated by the bond graph simulator and written in matrix form as follows.

$$\begin{pmatrix} v'_{C_2} \\ v'_{C_3} \\ v'_{C_4} \\ i'_{rec} \\ i'_{tcoil} \end{pmatrix} = \begin{bmatrix} 0 & 0 & 0 & 0 & \frac{1}{C_2} \\ 0 & -\frac{R_5+R_{vc}+8R_{tc}}{C_3R_{tc}(R_5+R_{vc})} & \frac{-8}{C_3(R_5+R_{vc})} & 0 & \frac{R_6(R_5+R_{vc}-23.2R_{tc})}{4C_3R_{tc}(R_5+R_{vc})} \\ 0 & \frac{-8}{C_4(R_5+R_{vc})} & \frac{-8}{C_4(R_5+R_{vc})} & 0 & \frac{-5.9R_6}{C_4(R_5+R_{vc})} \\ 0 & \frac{305.1}{I_{rec}} & \frac{305.1}{I_{rec}} & -\frac{R_{rec}}{I_{rec}} & \frac{225.9R_6}{I_{rec}} \\ \frac{-1}{I_{tcoil}} & 0 & 0 & 0 & \frac{-1.738R_6}{I_{tcoil}} \end{bmatrix} \begin{pmatrix} v_{C_2} \\ v_{C_3} \\ v_{C_4} \\ i_{rec} \\ i_{tcoil} \end{pmatrix} + \begin{pmatrix} 0 \\ 0 \\ 0 \\ 0 \\ \frac{MS_e}{I_{tcoil}} \end{pmatrix} \quad (1)$$

Here  $u'$  denotes a derivative of  $u$  with respect to time and numerical values represent the substitution of numerical constants such as amplifier gain and battery voltage in the model. A member of the ODE suite of codes in MATLAB [19] was modified to solve the dynamic system (1) and this solution was compared against that of bond graph software simulator [18] to validate the accuracy of the extracted linear equation system. The accuracy of the bond graph representation has already been validated against experimental results in [5] for the microphone mode.

### 3 Sensitivity and Uncertainty Analysis

#### 3.1 General Theory

First order dynamic differential models such as (1), linear or otherwise, take the general form

$$\frac{dy}{dt} = f(y, \theta, t) \quad (2)$$

where  $t$  represents time,  $y$  and  $\theta$  represent the vectors containing the  $n$  system outputs (solutions) and  $m$  parameters respectively, and  $f$  is a vector of functions in  $y$ ,  $\theta$  and  $t$  such that  $y = [y_1, y_2, \dots, y_n]^T$ ,  $\theta = [\theta_1, \theta_2, \dots, \theta_m]^T$  and  $f = [f_1, f_2, \dots, f_n]^T$ . Note that when  $f(y, \theta, t)$  can be broken into a pure state and a forcing input, as in the present case, we may write  $f(y, \theta, t) = \tilde{f}(y, \theta, t) + u(\theta, t)$ . Taking derivatives with respect to  $\theta$  on either side of the governing equations (2) results in the sensitivity differential equations

$$\frac{dS(\theta, t)}{dt} = \frac{\partial f}{\partial y} S(\theta, t) + \frac{\partial f}{\partial \theta} \quad (3)$$

which describe the time evolution of the  $n \times m$  local sensitivity matrix  $S(\theta, t)$  whose components are given by

$$S_{ij} = \frac{\partial y_i(\theta, t)}{\partial \theta_j} \quad (4)$$

The components (4) are termed local sensitivity coefficients. In (3), the  $n \times n$  matrix  $\frac{\partial f}{\partial y}$  and  $n \times m$  matrix  $\frac{\partial f}{\partial \theta}$  can be derived explicitly from (2) and are termed the Jacobian and parametric Jacobian matrices respectively.

By the direct method for sensitivity analysis [20] [21] the sets of differential equations (2) and (3) are solved jointly at each time step of a numerical time integration scheme, with information generated in the solution of (2) used in the solution of (3). Accordingly a solution to both  $y(\theta, t)$  and  $S(\theta, t)$  is returned at each time step of the numerical method. In the work presented here a member of the ODE suite of codes *ode45* [22] in MATLAB was modified to solve the governing and sensitivity differential equation system in this way.

Whilst numerical methods are not necessarily required to solve a linear governing system, the direct method as outlined here is readily extendable to

more complex non-linear models. At any time point  $t_0$  during the numerical solution process, based on a first order Taylor series approximation [23], the covariance of the system output vector  $\text{cov}(y)$  can be approximated by

$$\text{cov}(y(t_0)) \approx S(\mu_\theta, t_0)\Sigma_\theta S^T(\mu_\theta, t_0) \quad (5)$$

where  $\Sigma_\theta$  is the covariance matrix based on the predetermined variability in the system parameters and  $\mu_\theta$  is the vector of nominal parameter values. For independent system parameters  $\theta_i$  such that

$$\Sigma_\theta = \text{diag}(\sigma^2(\theta_1), \dots, \sigma^2(\theta_m)) \quad (6)$$

a linear estimate of  $\sigma^2(y_i(t_0))$ , the variance of model output  $y_i$  at  $t_0$  owing to parameter variability, can be written from (5) as

$$\sigma^2(y_i(t_0)) = \sum_{j=1}^m \sigma_j^2(y_i) \quad (7)$$

where  $\sigma^2(y_i(t_0))$  represents the diagonal elements of  $\text{cov}(y(t_0))$ , and

$$\sigma_j^2(y_i) \approx S_{ij}^2(\mu_\theta, t_0)\sigma^2(\theta_j) \quad (8)$$

is the contribution of the variance  $\sigma^2(\theta_j)$  in parameter  $\theta_j$  to the resultant variance in model output  $y_i$  at  $t_0$ . Therefore, the total output variance represented in equation (7) is a sum over independent parameter contributions.

### 3.2 Telecoil Sensitivity Formulation

Following on from the theory in section 3.1, for the telecoil system the state and parameter vectors are given from Tables 1 and 2 respectively by

$$y = [v_{C_2}, v_{C_3}, v_{C_4}, i_{rec}, i_{tcoil}]^T \quad (9)$$

$$\theta = [I_{tcoil}, R_6, I_{rec}, R_{rec}, C_2, C_4, R_5, R_{vc}, C_3, R_{tc}]^T \quad (10)$$

and the functions contained in the vector  $f$  of equation 2 are defined by the matrix-vector multiplication on the right hand side of (1).

The parametric Jacobian matrix in equation (3) is thus defined as

$$\frac{\partial f}{\partial \theta} = \begin{bmatrix} 0 & 0 & 0 & 0 & \frac{\partial v'_{C_2}}{\partial C_2} & 0 & 0 & 0 & 0 & 0 \\ 0 & \frac{\partial v'_{C_3}}{\partial R_6} & 0 & 0 & 0 & 0 & \frac{\partial v'_{C_3}}{\partial R_5} & \frac{\partial v'_{C_3}}{\partial R_{vc}} & \frac{\partial v'_{C_3}}{\partial C_3} & \frac{\partial v'_{C_3}}{\partial R_{tc}} \\ 0 & \frac{\partial v'_{C_4}}{\partial R_6} & 0 & 0 & 0 & \frac{\partial v'_{C_4}}{\partial C_4} & \frac{\partial v'_{C_4}}{\partial R_5} & \frac{\partial v'_{C_4}}{\partial R_{vc}} & 0 & 0 \\ 0 & \frac{\partial i'_{rec}}{\partial R_6} & \frac{\partial i'_{rec}}{\partial I_{rec}} & \frac{\partial i'_{rec}}{\partial R_{rec}} & 0 & 0 & 0 & 0 & 0 & 0 \\ \frac{\partial i'_{tcoil}}{\partial I_{tcoil}} & \frac{\partial i'_{tcoil}}{\partial R_6} & 0 & 0 & 0 & 0 & 0 & 0 & 0 & 0 \end{bmatrix} \quad (11)$$

whose elements should not be taken literally, but can be derived analytically from (1) as presented in Appendix A (known zeros are indicated). Owing to system linearity, the Jacobian  $\frac{\partial f}{\partial y}$  for the hearing aid system is equivalent to the system matrix in (1).

Solving the formulated sensitivity equation in the form of (3) alongside the governing system (1) returns the values of the system solution variables at each time step along side the sensitivity coefficients of equation (4) which form system sensitivity matrix given in this application by

$$S(\mu_\theta, t) = \begin{bmatrix} \frac{\partial v_{C_2}}{\partial I_{tcoil}} & \frac{\partial v_{C_2}}{\partial R_6} & \frac{\partial v_{C_2}}{\partial I_{rec}} & \frac{\partial v_{C_2}}{\partial R_{rec}} & \frac{\partial v_{C_2}}{\partial C_2} & \frac{\partial v_{C_2}}{\partial C_4} & \frac{\partial v_{C_2}}{\partial R_5} & \frac{\partial v_{C_2}}{\partial R_{vc}} & \frac{\partial v_{C_2}}{\partial C_3} & \frac{\partial v_{C_2}}{\partial R_{tc}} \\ \frac{\partial v_{C_3}}{\partial I_{tcoil}} & \frac{\partial v_{C_3}}{\partial R_6} & \frac{\partial v_{C_3}}{\partial I_{rec}} & \frac{\partial v_{C_3}}{\partial R_{rec}} & \frac{\partial v_{C_3}}{\partial C_2} & \frac{\partial v_{C_3}}{\partial C_4} & \frac{\partial v_{C_3}}{\partial R_5} & \frac{\partial v_{C_3}}{\partial R_{vc}} & \frac{\partial v_{C_3}}{\partial C_3} & \frac{\partial v_{C_3}}{\partial R_{tc}} \\ \frac{\partial v_{C_4}}{\partial I_{tcoil}} & \frac{\partial v_{C_4}}{\partial R_6} & \frac{\partial v_{C_4}}{\partial I_{rec}} & \frac{\partial v_{C_4}}{\partial R_{rec}} & \frac{\partial v_{C_4}}{\partial C_2} & \frac{\partial v_{C_4}}{\partial C_4} & \frac{\partial v_{C_4}}{\partial R_5} & \frac{\partial v_{C_4}}{\partial R_{vc}} & \frac{\partial v_{C_4}}{\partial C_3} & \frac{\partial v_{C_4}}{\partial R_{tc}} \\ \frac{\partial i_{rec}}{\partial I_{tcoil}} & \frac{\partial i_{rec}}{\partial R_6} & \frac{\partial i_{rec}}{\partial I_{rec}} & \frac{\partial i_{rec}}{\partial R_{rec}} & \frac{\partial i_{rec}}{\partial C_2} & \frac{\partial i_{rec}}{\partial C_4} & \frac{\partial i_{rec}}{\partial R_5} & \frac{\partial i_{rec}}{\partial R_{vc}} & \frac{\partial i_{rec}}{\partial C_3} & \frac{\partial i_{rec}}{\partial R_{tc}} \\ \frac{\partial i_{tcoil}}{\partial I_{tcoil}} & \frac{\partial i_{tcoil}}{\partial R_6} & \frac{\partial i_{tcoil}}{\partial I_{rec}} & \frac{\partial i_{tcoil}}{\partial R_{rec}} & \frac{\partial i_{tcoil}}{\partial C_2} & \frac{\partial i_{tcoil}}{\partial C_4} & \frac{\partial i_{tcoil}}{\partial R_5} & \frac{\partial i_{tcoil}}{\partial R_{vc}} & \frac{\partial i_{tcoil}}{\partial C_3} & \frac{\partial i_{tcoil}}{\partial R_{tc}} \end{bmatrix} \quad (12)$$

where each of the coefficients in (12) are calculated at  $\mu_\theta$  and at time  $t$ , where  $\mu_\theta$  is determined using the nominal values of the system parameters. The parameter nominal values and manufacturing tolerances for the hearing aid design were taken from the manufacturers data sheets and are presented in Table 2. Each manufacturing tolerance acts as a source of variability that is translated to variation in the system output. Parameter standard deviation was computed by assuming all parameter values are uniformly distributed within the prescribed range and using the standard formula  $\sigma = (b-a)/(2\sqrt{3})$ , where  $a$  and  $b$  are the lower and upper bounds, respectively.

| parameter  | description               | nominal        | tolerance  | Std. Dev.      |
|------------|---------------------------|----------------|------------|----------------|
| $R_5$      | resistance R5             | 6800 $\Omega$  | $\pm 10\%$ | 392.6 $\Omega$ |
| $R_6$      | resistance R6             | 75000 $\Omega$ | $\pm 5\%$  | 2165 $\Omega$  |
| $R_{rec}$  | receiver resistance       | 500 $\Omega$   | $\pm 10\%$ | 28.87 $\Omega$ |
| $R_{tc}$   | tone control resistance   | 1700 $\Omega$  | $\pm 10\%$ | 98.14 $\Omega$ |
| $R_{vc}$   | volume control resistance | 50000 $\Omega$ | $\pm 20\%$ | 5774 $\Omega$  |
| $C_2$      | capacitance C2            | 100e-09 F      | $\pm 5\%$  | 2.887e-09 F    |
| $C_3$      | capacitance C3            | 15e-09 F       | $\pm 10\%$ | 0.866e-09 F    |
| $C_4$      | capacitance C4            | 0.47e-06 F     | +80% -20%  | 0.137e-06 F    |
| $I_{rec}$  | receiver inductance       | 0.345 H        | $\pm 22\%$ | 0.0438 H       |
| $I_{coil}$ | telecoil inductance       | 0.295 H        | $\pm 15\%$ | 0.0255 H       |

Table 2

Hearing aid system parameter descriptions, manufacturing data for nominal values and tolerances and calculated standard deviations assuming Uniform distribution.

Using the sensitivity matrix (12) variations in parameter value can be propagated through to the system output using equations (7) and (8), with the individual sources contributing most to the output variance being identified by (8). The results of numerically implementing this strategy for determining the sources of variability in the hearing aid system model output are presented in Section 4.

## 4 Numerical Results

From the system outputs listed in Table 1, the currents  $i_{rec}$  and  $i_{coil}$  are investigated in terms of their sensitivity to other circuit component values since, in telecoil mode, the telecoil and receiver are known to interact in close proximity [24]. At a sinusoidal input signal<sup>2</sup> of amplitude 1mV and frequency 1 kHz, the simulated solutions  $i_{rec}$  and  $i_{coil}$  generated by solving the governing differential system (1) using a time integration scheme are also 1 kHz sinusoids

<sup>2</sup> This signal is equivalent to the expected input generated by a telecoil.

| parameter   | $\sigma_j(i_{rec})$ | $\sigma_j(i_{tcoil})$ |
|-------------|---------------------|-----------------------|
| $R_5$       | 0.09e-06            | 0                     |
| $R_6$       | 0.67e-06            | 224.3e-12             |
| $R_{rec}$   | 0.91e-06            | 0                     |
| $R_{tc}$    | 0.37e-06            | 0                     |
| $R_{vc}$    | 1.44e-06            | 0                     |
| $C_2$       | 0.02e-06            | 2.7e-12               |
| $C_3$       | 0.41e-06            | 0                     |
| $C_4$       | 0.78e-06            | 0                     |
| $I_{rec}$   | 8.79e-06            | 0                     |
| $I_{tcoil}$ | 0.09e-06            | 28.7e-12              |

Table 3

Individual parameter contribution to output sensitivity, expressed as standard deviations (Amperes per unit change of  $j$ th parameter).

of varying amplitudes with a d.c. offset. The system sensitivity coefficients will also be periodic at the same frequency since the governing and sensitivity equation systems share the same eigenvalues. By using the system sensitivity coefficients computed at each step of the solution procedure, the parameter variances were propagated through to the chosen model outputs. The peak-to-peak amplitudes of the simulated sinusoid solutions  $i_{rec}$  and  $i_{tcoil}$ , and their corresponding variances due to variation in parameter values are presented in Tables 3 and 4.

The output variance in  $i_{tcoil}$  was found to be mostly due to the variance of  $R_6$ , although this variance is negligible compared to the nominal output value of  $i_{tcoil}$ . As such  $i_{tcoil}$  can be considered robust to parameter variations. The major contributor to the variance in  $i_{rec}$  was seen to be that of parameter  $I_{rec}$  alongside small contributions from parameters  $R_{vc}$ ,  $R_{rec}$ ,  $C_4$  and  $R_6$ . As such, manufacturing tolerances on the other parameters have little or no effect on system performance.

|                            |           |            |
|----------------------------|-----------|------------|
| Nominal Pk-Pk Output Value | 0.625e-03 | 0.1013e-06 |
| Total Output Std. Dev.     | 13.63e-06 | 255.8e-12  |

Table 4

Peak-to-peak amplitudes of the 1kHz sinusoids representing  $i_{rec}$ ,  $i_{tcoil}$ , and the corresponding total standard deviation owing to parameter variation. All units in Amperes.

## 5 Conclusions

An analytic bond graph sensitivity analysis based methodology for robustness evaluation in multi-physics engineering systems has been presented and implemented in the case of a BTE hearing aid device. The methodology uses a linearized state space formulation of a bond graph system to identify key parameters from a robustness perspective while avoiding the need to continually re-run simulations at changing parameter values at the expense of solving a coupled sensitivity differential equation at each simulation time step. These results identify the most significant hearing aid design parameters from a robustness perspective so that they can be selected to either maximise performance or reduce costs.

The methods presented here can be applied generally to dynamic engineering systems, but are especially useful in a multi-energy domain, where an entire system can be modelled and analyzed in a single simulation environment. The linearization of the system is valid around a specified working point and is performed symbolically when the original system contains differentiable functions. For nonlinear systems the linearization process, which involves manipulation of equations, will not be as simple as for linear systems. However, formulation and reduction will follow the same pattern analytically even if simulation packages such as 20-Sim are unable to do this at present. This consistency of approach is addressed in [25].

## Appendix A

The elements of the parametric Jacobian matrix of equation 11 are given by

$$\frac{\partial v'_{C_2}}{\partial C_2} = \frac{-i_{tcoil}}{C_2^2} \quad (13)$$

$$\frac{\partial v'_{C_3}}{\partial C_3} = \frac{v_{C_3}(8R_{tc} + R_5 + R_{vc}) + R_6 i_{tcoil}(5.8R_{tc} - 0.26(R_5 + R_{vc})) + 8R_{tc}v_{C_4}}{C_3^2 R_{tc}(R_5 + R_{vc})} \quad (14)$$

$$\frac{\partial v'_{C_3}}{\partial R_5} = \frac{\partial v'_{C_3}}{\partial R_{vc}} = \frac{8v_{C_3} + 8v_{C_4} + 5.9R_6 i_{tcoil}}{C_3(R_5 + R_{vc})^2} \quad (15)$$

$$\frac{\partial v'_{C_3}}{\partial R_{tc}} = \frac{v_{C_3} - (R_6 i_{tcoil})/4}{C_3 R_{tc}^2} \quad (16)$$

$$\frac{\partial v'_{C_3}}{\partial R_6} = \frac{-5.9i_{tcoil}}{C_3(R_5 + R_{vc})} \quad (17)$$

$$\frac{\partial v'_{C_4}}{\partial C_4} = \frac{(8v_{C_3} + 8v_{C_4} + 5.9R_6 i_{tcoil})}{C_4^2(R_5 + R_{vc})} \quad (18)$$

$$\frac{\partial v'_{C_4}}{\partial R_5} = \frac{\partial v'_{C_4}}{\partial R_{vc}} = \frac{8v_{C_3} + 8v_{C_4} + 5.9R_6 i_{tcoil}}{C_4(R_5 + R_{vc})^2} \quad (19)$$

$$\frac{\partial v'_{C_4}}{\partial R_6} = \frac{-5.9i_{tcoil}}{C_4(R_5 + R_{vc})} \quad (20)$$

$$\frac{\partial i'_{rec}}{\partial I_{rec}} = \frac{1}{I_{rec}^2}(-305v_{C_3} - 305v_{C_4} + R_{rec}i_{rec} - 226R_6 i_{tcoil}) \quad (21)$$

$$\frac{\partial i'_{rec}}{\partial R_{rec}} = \frac{-i_{rec}}{I_{rec}} \quad (22)$$

$$\frac{\partial i'_{rec}}{\partial R_6} = \frac{226i_{tcoil}}{I_{rec}} \quad (23)$$

$$\frac{\partial i'_{tcoil}}{\partial I_{tcoil}} = \frac{1}{I_{tcoil}^2}(v_{C_2} + 1.73i_{tcoil}R_6 - MS_e) \quad (24)$$

$$\frac{\partial i'_{tcoil}}{\partial R_6} = \frac{-1.73i_{tcoil}}{I_{tcoil}} \quad (25)$$

## Acknowledgements

The authors wish to thank Siemens Hearing Instruments Ltd, Crawley, UK for access to their hearing aid manufacturing data. This work was supported by the Engineering & Physical Sciences Research Council (EPSRC) at the London School of Economics under grant number GR/S63502/01 and at Brunel University under grant number GR/S63496/02.

## References

- [1] J. Wu and M. Hamada. *Experiments: Planning, Analysis, and Parameter Design Optimization*. Wiley, 2000.
- [2] D. M. Grove and T. P. Davis. *Engineering, Quality and Experimental Design*. Longman, 1992.
- [3] T.R. Hsu. *MEMS and Microsystems: Design and Manufacture*. McGraw-Hill Company, Boston, 2002.
- [4] B. Shield. Evaluation of the social and economic costs of hearing impairment. *www.hearit.org*, 2005.
- [5] M. A. Atherton, R.A. Bates, D. Ashdown, and F. Jensen. Evaluating hearing aid robustness using bond graph models. *Proc. of Mechatronics 2002, 24-26 June, Enchede, Netherlands*, pages 591–597, 2002.
- [6] H. Kim and D. Barrs. Hearing aids: A review of whats new. *Otolaryngology - Head and neck surgery*, 134:1043–1050, 2006.
- [7] J. Gao, H. Zhang, and G. Hu. Real time implementation of an efficient speech enhancement algorithm for digital hearing aids. *Tsinghua Science and Technology*, 11(2):475–480, 2006.
- [8] H. Puder. Adaptive signal processing for interference cancellation in hearing aids. *Signal Processing*, 86:1239–1253, 2006.
- [9] J-B. Maj, L. Royackers, J. Wouters, and M. Moonen. Comparison of adaptive noise reduction algorithms in dual microphone hearing aids. *Speech Communication*, 48:957–970, 2006.
- [10] H.M. Paynter. *Analysis and Design of Engineering Systems*. MIT Press, Cambridge, MA., 1961.
- [11] D.C. Karnopp. Computer simulation of stick-slip friction in mechanical dynamic systems. *Transcripts of ASME Journal of Dynamic Systems, Measurement, and Control*, 107(1):100–103, 1985.
- [12] R.C. Rosenberg. Exploiting bond graph causality in physical systems models. *Journal of Dynamic Systems, Measurement, and Control*, 109(4):378–383, 1987.
- [13] F.E. Cellier. Hierarchical nonlinear bond graphs: a unified methodology for modelling complex physical systems. *Proceedings of European Simulation Multiconference on Modelling and Simulation*, pages 1–3, 1990.

- [14] D.C. Karnopp. Energetically consistent bond graph models in electromechanical energy conversion. *Journal of the Franklin Institute*, 325(7):667–686, 1990.
- [15] M.A. Atherton and R.A. Bates. Bond graph analysis in robust engineering design. *Quality and Reliability Engineering International*, 16:325–335, 2000.
- [16] P. J. Gawthrop. Sensitivity bond graphs. *Journal of the Franklin Institute*, 227:907–922, 2000.
- [17] W. Barutski and J. Granda. Bond graph based frequency domain sensitivity analysis of multidisciplinary systems. *Proceedings of the I MECH E Part I: Journal of Systems & Control Engineering*, 216(1):85–99, 2002.
- [18] Controllab Products B. V. <http://www.20sim.com>.
- [19] L. F. Shampine and M. W. Reichelt. The matlab ode suite. *Siam Journal of Scientific Computing*, 18(1):1–22, 1997.
- [20] J. R. Leis and M. A. Kramer. The simultaneous solution and sensitivity analysis of systems described by ordinary differential equations. *ACM Transactions on Mathematical Software*, 14(1):45–60, 1988.
- [21] A. M. Dunker. The decoupled direct method for calculating sensitivity coefficients in chemical kinetics. *J. Chem. Phys.*, 81:2385–2393, 1984.
- [22] L. F. Shampine and M. W. Reichelt. The matlab ode suite. *Siam J. Sci. Comput.*, 18(1):1–22, 1997.
- [23] Dan G. Cacuci. *Sensitivity and Uncertainty Analysis Theory*. Chapter 3, Chapman and Hall/CRC, 2003.
- [24] Y. Shen, M. A. Perry, E. Kaymak, M. A. Atherton, R. A. Bates, and H. P. Wynn. Experimental and bond graph based sensitivity calculations for micro scale robust engineering design. *Annecy, France 2005: Research and Education in Mechatronics*, pages CD-ROM, 2005.
- [25] D.C. Karnopp, D.L. Margolis, and R.C. Rosenberg. *System Dynamics*, pages 138–142. Wiley Interscience, 1990.